

Supplementary information

**Ordered mesoporous silica framework based electrolyte
with nanowetted interfaces for solid-state lithium batteries**

Lei Han, Ziqi Wang*, Defei Kong, Luyi Yang, Kai Yang, Zijian Wang, and Feng
Pan*

School of Advanced Materials, Peking University Shenzhen Graduate School,
Shenzhen 518055, China.

* Corresponding author: wangzq@pkusz.edu.cn

panfeng@pkusz.edu.cn

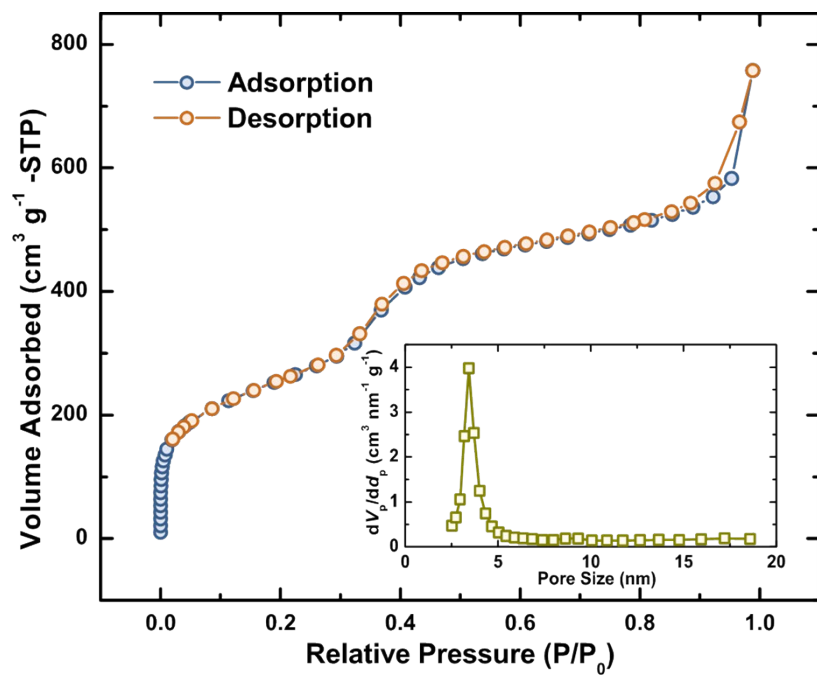


Fig. S1 N₂ adsorption/desorption isothermal of pristine MCM-41, inset: BJH pore size distribution plot.

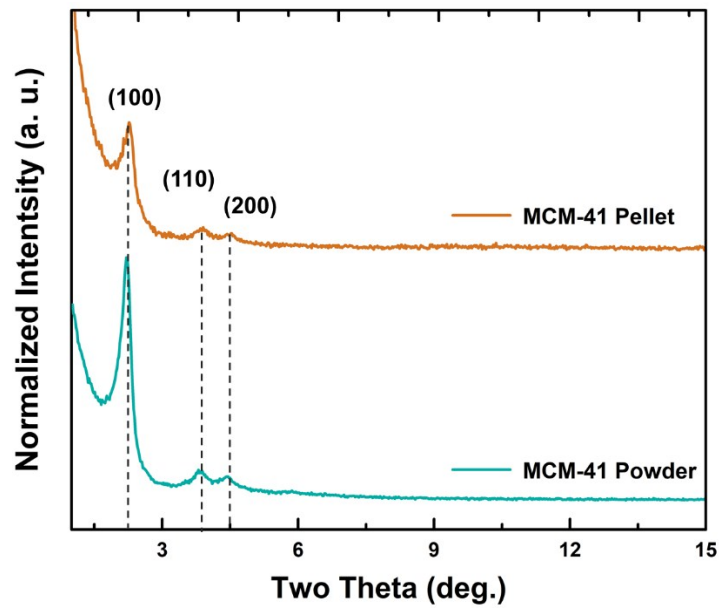


Fig. S2 XRD patterns of MCM-41 powder and pellet.

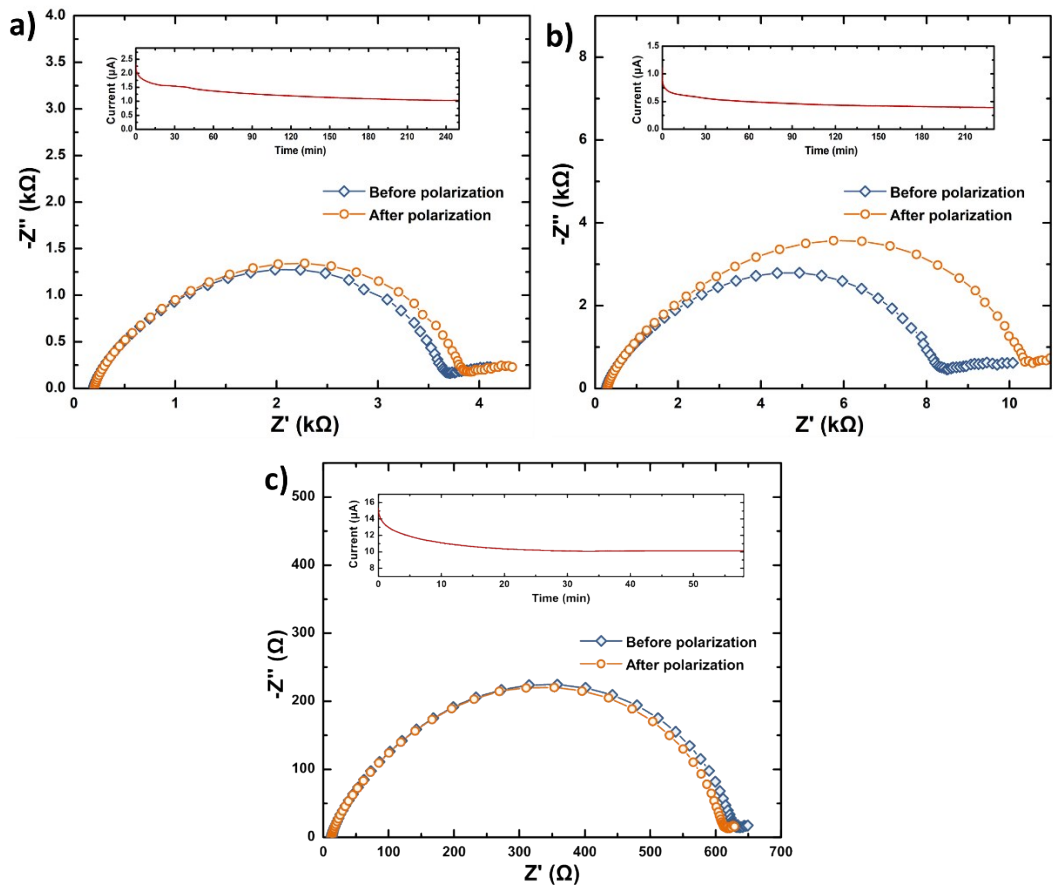


Fig. S3 EIS of a) Li|Li-IL@MCM-41 (2.0 mL@1g) |Li, b) Li|Li-IL@MCM-41 (1.7 mL@1g) |Li and c) Li|Li-IL|Li symmetric cells before and after the DC polarization under room temperature. Inset: time-dependent current response of DC polarization for the symmetric cells.

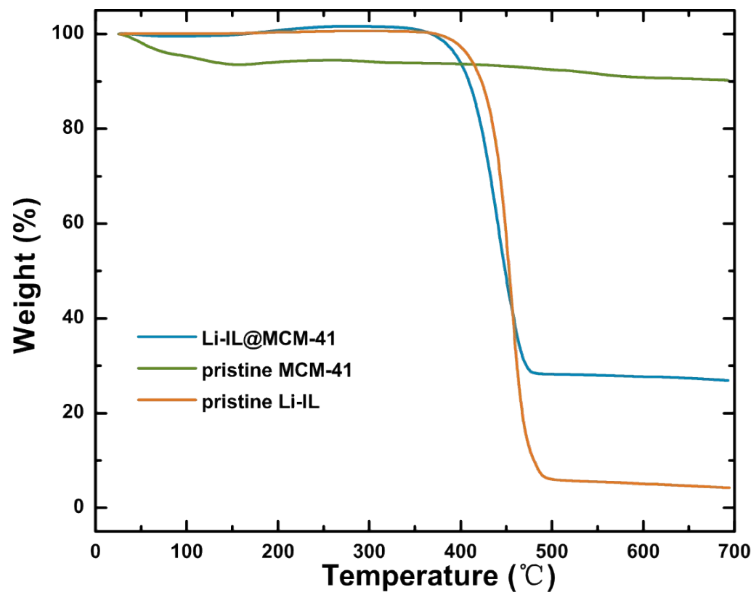


Fig. S4 TAG profiles of Li-IL@MCM-41, pristine Li-IL and pristine MCM-41 from room temperature to 700 °C at a speed of 10 °C min⁻¹ under a N₂ flow.

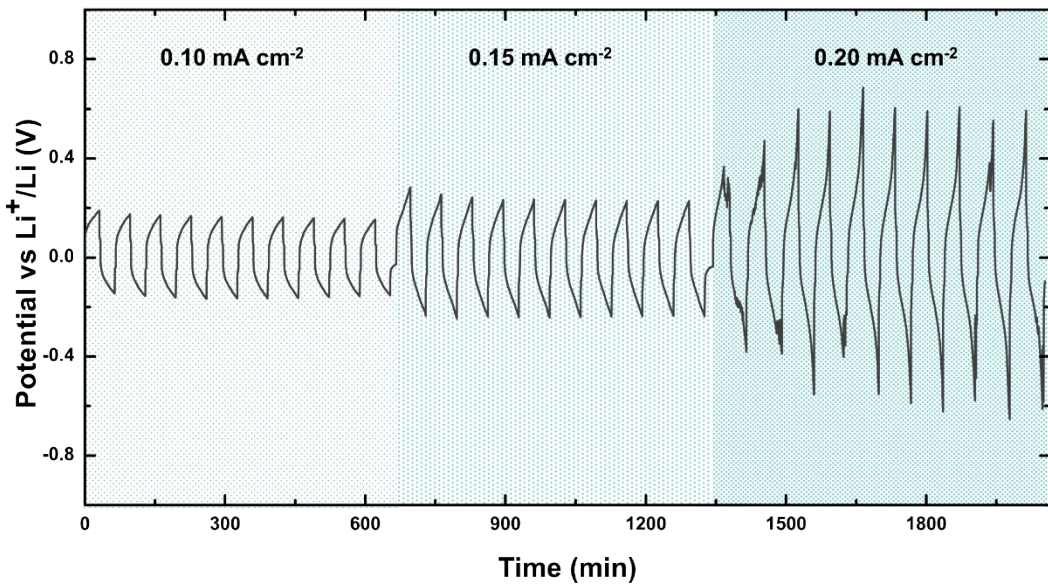


Fig. S5 Voltage profiles for Li||Li-IL@MCM-41||Li symmetric cell at current density of 0.10, 0.15 and 0.20 mA cm⁻².

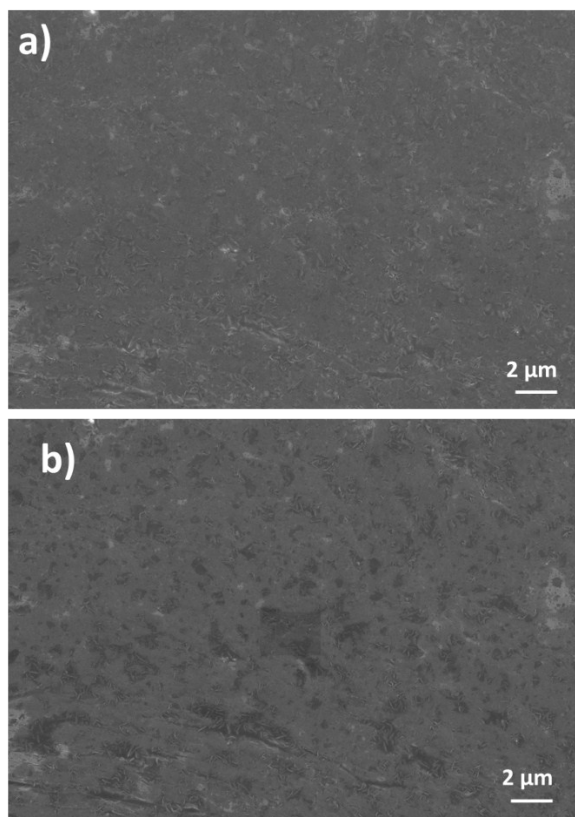


Fig. S6 SEM morphology of the Li metal surface after Li plating/stripping cycles a) before and b) after several minutes of electron bombardment.

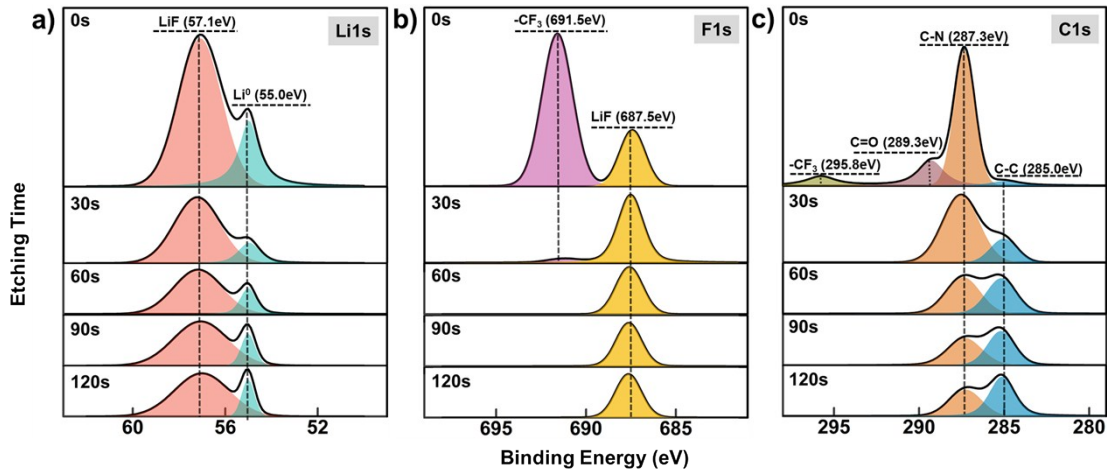


Fig. S7 XPS spectra for a) Li1s, b) F1s and c) C1s from the lithium metal electrode after Li plating/stripping cycles.

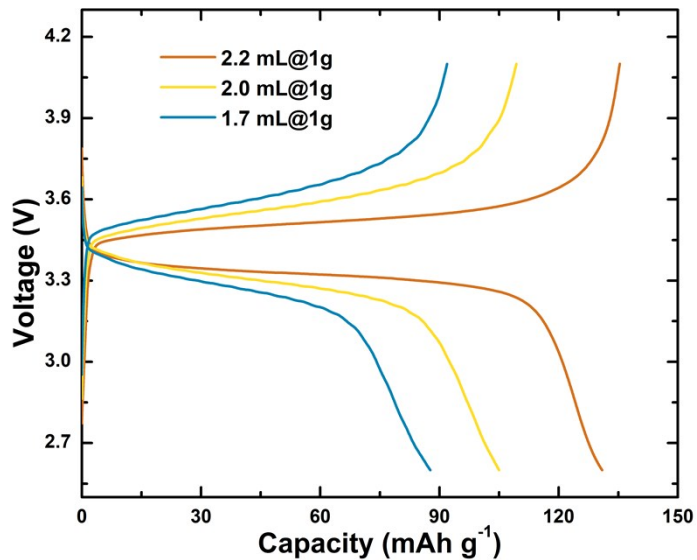


Fig. S8 Charge/discharge curves of Li|Li-IL@MCM-41|LFP SSB at 0.1 C under room temperature with different occupancy rate.

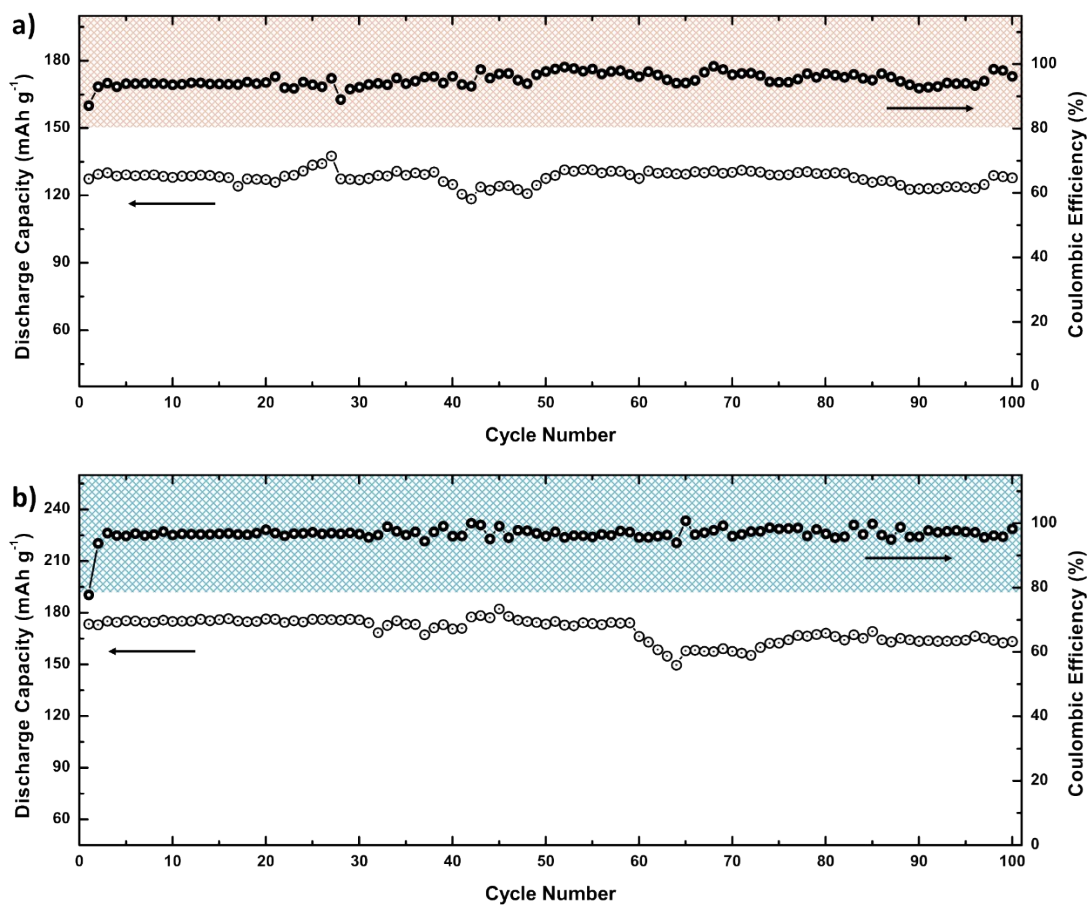


Fig. S9 a) Cycling performance of $\text{Li}|\text{Li-IL}@\text{MCM-41}|\text{LCO}$ SSB at 0.1 C rate under room temperature. b) Cycling performance of $\text{Li}|\text{Li-IL}@\text{MCM-41}|\text{NCM}$ SSB at 0.1 C rate under room temperature.

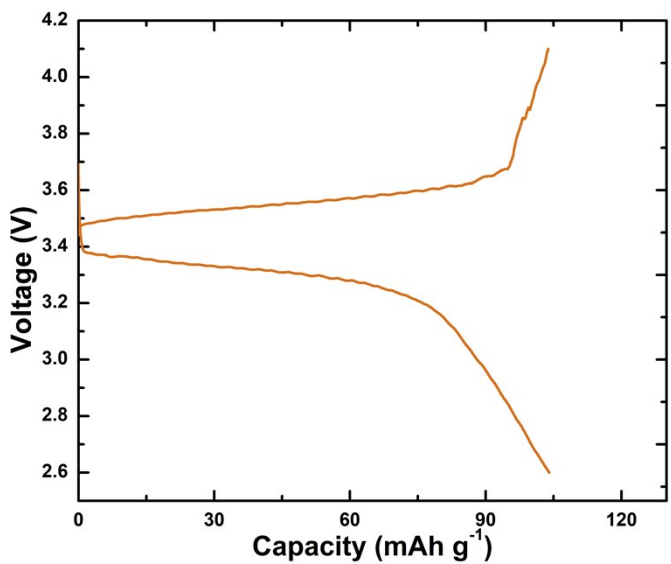


Fig. S10 Charge/discharge curve of Li|Li-IL@MCM-41|LFP SSB at 0.1 C under room temperature with active loading of 6.1 mg cm^{-2} .

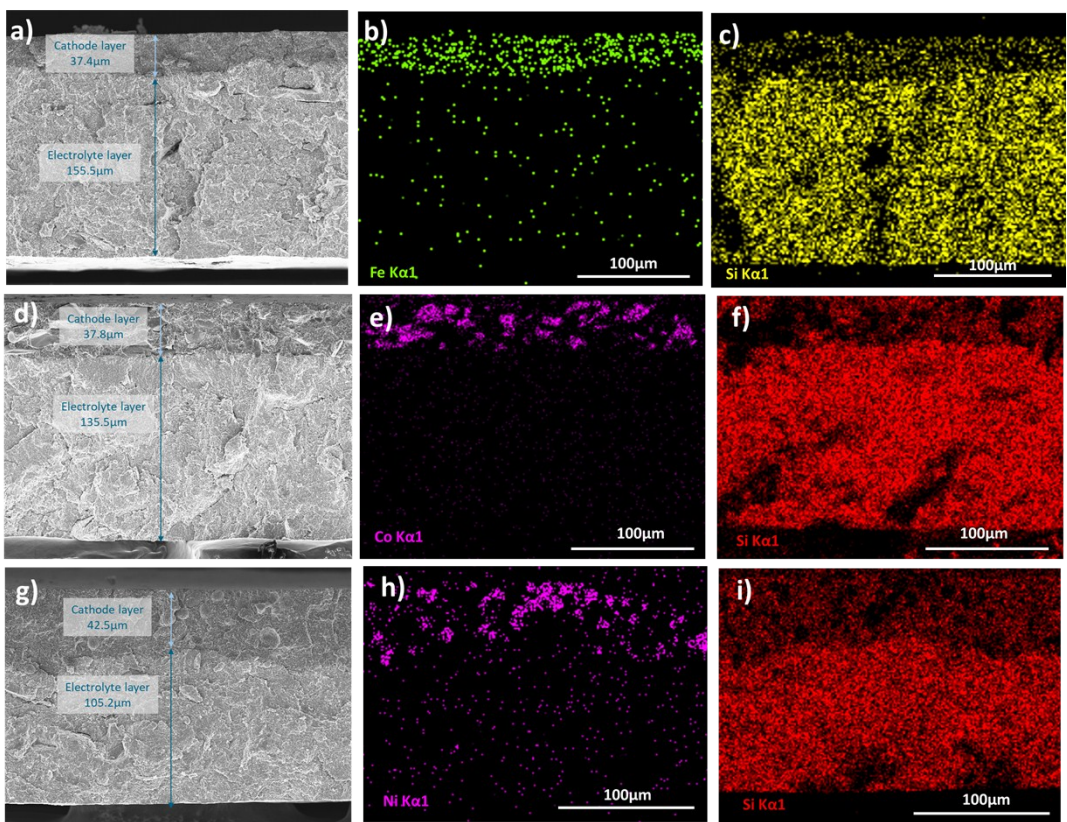


Fig. S11 a) SEM morphology of the cross section of Li-IL@MCM-41|LFP double-layer structure and b, c) corresponding EDS elemental mappings. d) SEM morphology of the cross section of Li-IL@MCM-41|LCO double-layer structure and e, f) corresponding EDS elemental mappings. g) SEM morphology of the cross section of Li-IL@MCM-41|NCM double-layer structure and h, i) corresponding EDS elemental mappings.

Tab. S1 Calculation of the specific energy and energy density of Li|Li-IL@MCM-41|LFP SSB.

Design parameter	Material	Thickness (μm)	Mass ($\text{mg}\cdot\text{cm}^{-2}$)	Mass ratio (%)
Anode current collector	None	0	0	0
Cathode current collector ^[1]	Al foil	5	1.34	6.6
Cathode	Active material	80	14.6	29.9 (104 mAh g ⁻¹ , experimental)
	Li-IL@MCM-41			29.9
	Acetylene black			12.1
Solid-state electrolyte	Li-IL@MCM-41	20	3.56	17.5
Anode (400% excess) ^[2]	Li metal	15	0.8	4 (3860 mAh g ⁻¹ , estimated)
Total	--	149	20.3	100
Calculated result	Energy density: 142.8 Wh L⁻¹ Specific energy: 105.0 Wh kg⁻¹			

Tab. S2 Comparison of battery performance and electrochemical properties between Li-IL@MCM-41 SSE and the recently reported ones.

SSE	Electrochemical window (V)	Conductivity (RT mS·cm ⁻¹)	Cathode materials	Initial discharge capacity	Capacity retention (%)	Cycle number	Date	Ref.
Li-IL@MCM-41	0–5.2	0.4	LiNi _{0.8} Co _{0.1} Mn _{0.1} O ₂	173	94	100	2018	This work
			LiCoO ₂	127	100	100		
			LiFePO ₄	138	100	100		
CPOSS-IL	-0.65–4.6	0.12	LiFePO ₄	121	92	100	2017	3
LLZTO-2wt.% Li ₃ OCl	>10	0.227	LiFePO ₄	75	200	100	2018	4
Li(BH ₄) _{1-x} (NH ₂) _x	0.7–2.0	6.7	-	-	-	-	2017	5
Li-IL@MOF	2–4.1	0.3	LiFePO ₄	145	90	100	2017	6
POSS-IL	1.4–5	0.48	LiFePO ₄	154	94	65	2017	7
LLCZNO	-	0.22	Sulfur	645	73	35	2017	2
Li ₇ P ₂ S ₈ I	-	1.35	LiNi _{0.6} Co _{0.2} Mn _{0.2} O ₂	175	74	40	2018	8

References

- 1 N. Chen, Y. Dai, Y. Xing, L. Wang, C. Guo, R. Chen, S. Guo and F. Wu, *Energy Environ. Sci.*, 2017, **10**, 1660–1667.
- 2 Kun (Kelvin) Fu, Y. Gong, G. T. Hitz, D. W. McOwen, Y. Li, S. Xu, Y. Wen, L. Zhang, C. Wang, G. Pastel, J. Dai, B. Liu, H. Xie, Y. Yao, E. D. Wachsman and L. Hu, *Energy Environ. Sci.*, 2017, **10**, 1568–1575.
- 3 G. Yang, H. Oh, C. Chanthad and Q. Wang, *Chem. Mater.*, 2017, **29**, 9275–9283.
- 4 Y. Tian, F. Ding, H. Zhong, C. Liu, Y.-B. He, J. Liu, X. Liu and Q. Xu, *Energy Storage Mater.*, 2018, **14**, 49–57.
- 5 Y. Yan, R.-S. Kühnel, A. Remhof, L. Duchêne, E. C. Reyes, D. Rentsch, Z. Łodziana and C. Battaglia, *Adv. Energy Mater.*, 2017, **7**, 1700294.
- 6 Z. Wang, R. Tan, H. Wang, L. Yang, J. Hu, H. Chen and F. Pan, *Adv. Mater.*, 2017, **30**, 1704436.
- 7 G. Yang, C. Chanthad, H. Oh, I. A. Ayhan and Q. Wang, *J. Mater. Chem. A*, 2017, **5**, 18012–18019.
- 8 S.-J. Choi, S.-H. Choi, A. D. Bui, Y.-J. Lee, S.-M. Lee, H.-C. Shin and Y.-C. Ha, *ACS Appl. Mater. Interfaces*, 2018, **10**, 31404–31412.